inter.noise
21-24 AUGUST
SCOTTISH EVENT CAMPUS
GLASGOW
2022

Valve noise at high pressure ratios

Erika Quaranta[1] and Malcolm Smith[2]
ISVR Consulting
University of Southampton
Southampton, SO17 1BJ, UK

ABSTRACT

When high pressure air expands through an orifice it can be an intense noise source, which may be hazardous for nearby personnel if it occurs in an unexpected or uncontrolled way. This paper describes a set of measurements that were carried out to validate and calibrate a well-known semi-empirical prediction method. A number of valve mockups were tested over a range of mass flow rates with pressure ratios up to 11 Bar, so that the model could be used with confidence to extrapolate to higher pressures, larger valve sizes and higher mass flows.

Interpretation of the measured noise data is carried out using an isentropic analysis of the flow, assuming choked conditions in the orifice to infer a jet Mach number and mass flow rate for each test condition. Based on this inferred flow data the sound power scaled as expected with 8th power of jet Mach number.. It is also shown that for all valves the sound power varied as 1.5th power of mass flow rate in the higher range, which is in reasonable agreement with the law implicit in the semi-empirical model, and provided a good basis for extrapolating to larger devices.

1. INTRODUCTION

The noise of high pressure air expanding through an orifice, as occurs in blow-off and pressure release valves, can be an intense source of jet noise, which may be hazardous for nearby personnel.

Noise levels may be predicted using the valve noise model detailed by H. Heller and P. Franken in the reference textbook edited by Beranek [1], which describes three flow and noise source regimes as follows:

$M_{jet} < 1$	→ turbulent mixing noise;
$1 < M_{jet} < 1.5$	→ turbulent mixing noise + shock noise;
$M_{jet} > 1.5$	→ shock noise.

M_{jet} is defined as the Mach number at the valve exit, depending on the pressure ratio (PR) of the total over the ambient pressure P_{tot}/P_{amb} and ratio of specific heats γ, which is evaluated from the isentropic relation

[1] E.Quaranta@soton.ac.uk
[2] mgs@isvr.soton.ac.uk

$$M_{jet} = \sqrt{\frac{2}{\gamma - 1}\left[\left(\frac{P_{tot}}{P_{amb}}\right)^{\frac{\gamma-1}{\gamma}} - 1\right]} \quad (1)$$

In the first regime $M_{jet} < 1$, when the turbulent mixing is the prevalent noise mechanism, the ratio of acoustic power to mechanical stream power $W_{mec} = \frac{1}{2}\dot{m}\, u_{jet}^2$ is proportional to M_{jet}^5. This is because the mass flow rate $\dot{m}$ is linearly dependent on jet velocity u_{jet}, so that W_{mec} varies as u_{jet}^3, whereas the acoustic power of turbulent mixing noise increases as the 8th power of u_{jet}. The constant of proportionality depends on the ratio of jet density and temperature to ambient values. For ambient conditions the sound power level is

$$L_{mix}(\text{dB}) = 10 \log\left(5\text{e}\ 5\, M_{jet}^5\right) + L_{mec} \quad (2)$$

where $L_{mec} = 10 \log\left(\frac{W_{mec}}{W_{ref}}\right)$ and W_{ref} is 1e-12 W.

In the third regime M_{jet} >1.5 the shock noise is prevalent. The ratio of the overall sound power radiated to the mechanical stream power in dB is linear dependent on PR, but the slope depends on the M_{jet}range, being steeper for $M_{jet} < 2.5$ and much less steep for $M_{jet} > 2.5$.

The laws derived from the semi-empirical model are

$$L_{shock}(\text{dB}) = -40 + 37 \log\left(\frac{\text{PR}}{2}\right) + L_{mec} \quad \text{if} \quad \text{PR} < 2.5 \quad (3)$$

$$L_{shock}(\text{dB}) = -26 + 7 \log\left(\frac{\text{PR}}{2.5}\right) + L_{mec} \quad \text{if} \quad \text{PR} > 2.5 \quad (4)$$

where L_{mec} is evaluated for u_{jet} equal to the speed of sound.

However, when $1 < M_{jet} < 1.5$ both noise mechanisms must be included, and the total sound power is the resultant of the sum of the two contributions.

Whilst the noise model is well established for some applications, for the particular industrial noise problem under consideration there was a need for the model to be calibrated so it could be used with confidence to extrapolate to unusually high pressure ratios and flow rates.

2. METHODOLOGY FOR TESTING

2.1. Test rig

The flow noise rig was installed in the large anechoic chamber at the Institute of Sound and Vibration Research (ISVR). The chamber has a total volume of 295 m^3 and it is certified to be fully anechoic above 90 Hz. The ambient noise level inside the chamber is well below the noise floor of the instrumentation. During the measurements all doors of the chamber were fully closed.

The valves were securely attached to the end of a 1m long instrumented duct placed in the centre of the chamber. The other end of this duct was attached to a 15m long thick-walled rubber hose which provided the connection to test facility's 15 bar pressure reservoir through a remotely controllable valve.

A photograph of the test arrangement is shown in Figure 1, indicating how the duct and test valve were supported and the positioning of the microphones.

Figure 1: Test arrangement.

2.2. Acoustic Instrumentation and analysis

The main noise data were recorded using 5 Brüel & Kjær Type 4189 1/2 ” microphones. Four microphones were placed 3 m away from the centre of the valves at polar angular positions of 10°, 30°, 60° and 90°. A microphone at 0° was not possible due to the jet of air. The 5th microphone was placed opposite the 90° microphone position at an azimuthal angle of 180° to provide a symmetry comparison.

The microphones were all more than 1 metre away from the wedges of the anechoic chamber and also had windshields installed. For tests with a 90° bend in the valve the microphone array was moved to new equivalent positions since rotating the test rig was difficult.

The microphones were connected to a Brüel & Kjær Pulse system, which was connected to a laptop running Brüel & Kjær Labshop analyser software. A microphone calibrator was placed on each of the microphones in order to verify and calibrate the measurement system. The analyser was used to acquire both 4 Hz constant bandwidth autospectra and 1/3 Octave band data based on 30s long recordings for each microphone and test case.

The spectra are converted to sound pressure levels (SPL) in dB using:

$$\text{SPL} = 10 \log\left(\frac{p^2}{p_{ref}^2}\right) \tag{5}$$

where $p_{ref} = 20\text{e-}6$ Pa.

The microphones were calibrated at 1 kHz to 94 dB before the testing began. An RS temperature sensor was used to record the temperature inside the nozzle. The pressure sensors were used to measure the static and total pressure for each pressure ratio inside the nozzle.

Overall sound power levels radiated into the downstream hemisphere have been evaluated as

$$L_w = 10 \log\left(\sum_{i=1}^{4} \frac{p_i^2}{p_{ref}^2} A_i\right) \tag{6}$$

where the index *i* is over microphones 1 to 4 and A_i is the area of the spherical sector of radius *R*=3m relative to the microphone placed at the angle α_i, i.e.

$$A_i = 2\pi R^2[\cos(\alpha_i - \delta) - \cos(\alpha_i + \delta)]$$

where 2δ is the angle between two microphones, thus δ = 15°.

2.3. Test items

Tests were conducted on 6 valves, which were simplified mockups of actual production valves. The valves were chosen to have a range of sizes and both straight through and L-ported in order to verify and extend the valve model. The main characteristics of the components tested were:

Valve 1: A straight through valve with a 12.5 mm bore and an expansion to 20.9 mm outlet.

Valve 2: A straight through valve which was made from a pipe with internal diameter of 20.9 mm and a contraction to 13.5 mm screwed on the outlet.

Valve 3: L-ported 3 way valve represented as a uniform 26.6 mm diameter pipe with a radiused elbow and a flange at the end.

Valve 3a: A straight-through version of Valve 3.

Valve 5: L-ported valve of uniform diameter throughout, manufactured from a 48.7 mm internal diameter pipe, with a flange at the outlet.

Valve 6: L-ported valve of uniform diameter throughout, manufactured from a 54 mm internal diameter pipe, with a flange at the outlet.

3. ANALYSIS OF RESULTS

For each valve, the SPL was acquired at various values of total pressure P_{tot}, starting from a subsonic jet flow condition, and gradually increasing to achieve over 10 Bar. However, for valve 5 and 6, because of the higher mass flow rate, the maximum total pressure achieved was 8 and 6.7 Bar respectively.

In Table 1, estimated values of mass flow rate $\dot{m}_{exit}$ and jet Mach number M_{jet} are reported, for constant $T_{tot} = 300K$. They can only be accurately evaluated for choked conditions, i.e. M_{valve}=1 corresponding to pressure ratio greater than $\left(\frac{\gamma+1}{2}\right)^{\frac{\gamma}{\gamma-1}}$, when the exit flow conditions are known by isentropic flow equations [2], and from Eq. 1 as

$$P_{tot} = \left(\frac{\gamma+1}{2}\right)^{\frac{\gamma}{\gamma-1}} P_{exit} = 1.893\, P_{exit} \tag{7}$$

$$T_{tot} = T\left(1 + \frac{\gamma - 1}{2} M_{valve}^2\right) = 1.2\, T \tag{8}$$

$$u_{exit} = c = \sqrt{\gamma RT} \tag{9}$$

$$\rho = \frac{P}{\gamma RT} \tag{10}$$

$$\dot{m}_{exit} = \rho u_{exit} A = 0.04\, A\, \frac{P_{tot}}{\sqrt{T_{tot}}} \tag{11}$$

where

P_{exit} = pressure at the valve exit;

T_{tot} = total temperature in the tank;

T = static temperature;

ρ = density;

u_{exit} = velocity at the valve exit which is equivalent to the speed of sound *c*;

$A =$ throttle area;

$\gamma = 1.4$; $R = 287$ J/kg : gas constants for air.

Results of the overall sound power levels for each test condition are also presented in Table 1.

Table 1: Test matrix with calculated mass flow rate, jet Mach number and overall sound power level.

Valve No.	nozzle diameter D (mm)	$\frac{P_{tot}}{P_{amb}}$	$\dot{m}_{exit}$ (kg/s)	M_{jet}	Sound power (dB re 1pW)
1	12.5	1.39	-	0.70	111.9
		1.79	0.050	0.95	115.8
		2.45	0.069	1.20	122.0
		4.97	0.140	1.70	111.4
		8.74	0.246	2.07	128.3
		11.47	0.325	2.24	134.0
2	13.5	1.53	-	0.81	103.8
		1.85	0.061	0.98	110.3
		2.26	0.075	1.14	115.9
		5.97	0.197	1.82	134.0
		11.03	0.364	2.22	137.3
3	26.6	1.61	-	0.85	121.1
		2.09	0.269	1.08	126.4
		3.96	0.508	1.55	137.6
		5.31	0.681	1.75	142.0
		11.07	1.420	2.22	147.0
3a	26.6	1.42	-	0.73	108.3
		1.96	0.251	1.03	119.0
		4.39	0.564	1.62	141.0
		5.65	0.725	1.79	141.4
		10.38	1.332	2.18	144.9
5	48.7	1.58	-	0.84	127.5
		2.25	0.971	1.14	134.5
		3.81	1.647	1.53	143.6
		5.99	2.583	1.83	149.9
		8.04	3.470	2.02	151.7
6	54	1.52	-	0.80	127.1
		2.14	1.135	1.10	134.4
		3.72	1.978	1.51	144.6
		4.30	2.284	1.61	146.0
		5.37	2.851	1.76	150.1
		6.68	3.546	1.90	151.6

Some typical spectra for the microphone placed at 30° are presented in Figure 2. The peak frequency of subsonic jet noise would increase with velocity, as $f_{peak} = (S\, u_{exit})/D$ based on the Strouhal number (non-dimensional frequency) S = 0.2, while the shock noise spectrum for choked valves peaks at lower frequencies, as exit velocity does not increase over the speed of sound and the Strouhal number decreases with PR as reported in [1]. This is broadly confirmed by the experimental spectra, even if there is no significant shift in frequency especially for the higher PRs.

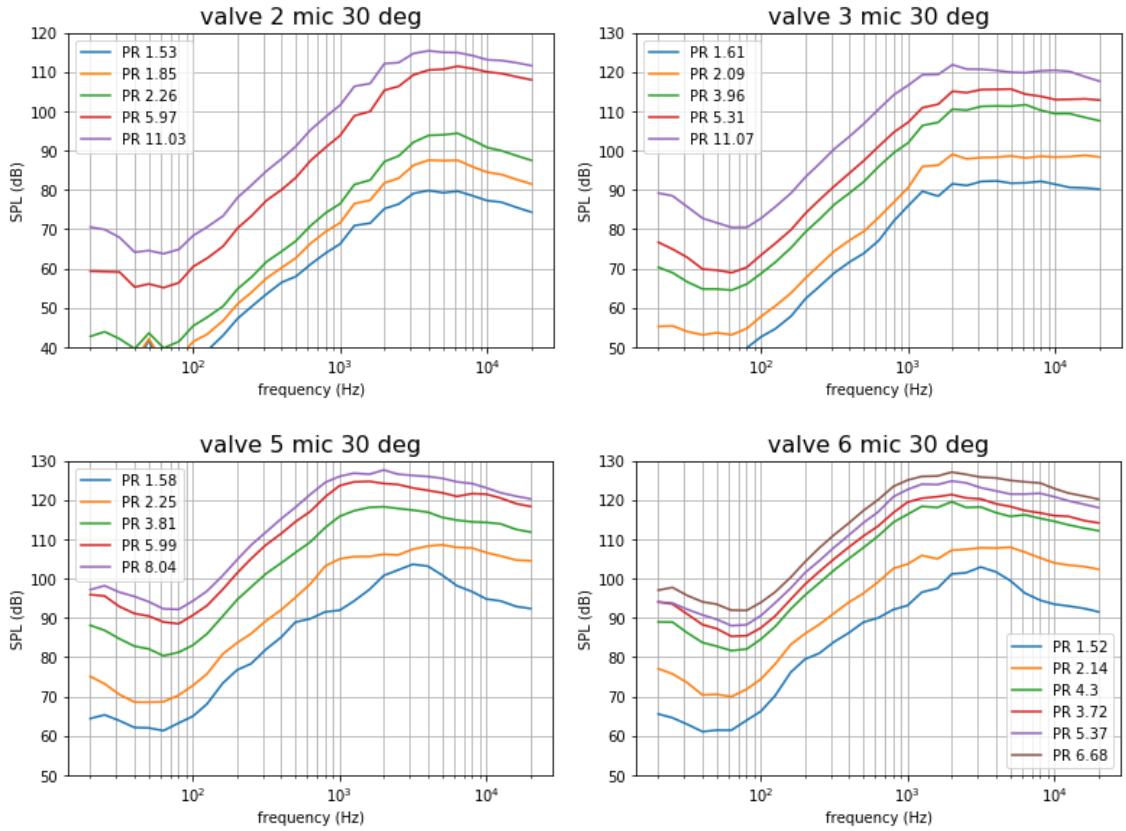

Figure 2: Sound spectra for the microphone at 30°.

4. COMPARISON WITH THE VALVE MODEL

The sound power levels have been compared with predicted values evaluated using the semi-empirical model proposed in Beranek [1] and explained in detail in the Section 1. Results were plotted versus PR (Figure 3), M_{jet} (Figure 4) and $\dot{m}_{exit}$ (Figure 5). The predicted levels were evaluated using different noise data laws depending on M_{jet}, therefore the lines have different slopes depending on the M_{jet} range.

Generally, noise level increases with the valve size, but results can be grouped in 3 sets: a) valve 1 and 2, b) valve 3 and 3a, c) valve 5 and 6. Variations within each set are negligible, suggesting that the global valve size is the overall dominant parameter, while detailed valve design does not significantly affect the noise level.

However, the anomaly of valve 1 might be due to the different design from the other valves. Valve 2, 3, 3a, 5 and 6 all have converging nozzles, while valve 1 nozzle was converging then diverging. This means that the throttle is not at the exit, but inside the valve, so that choking condition is at the throttle, but the flow in the jet is supersonic [2]. M_{jet} as defined for an isentropic expansion is not applicable. For increasing PR a normal shock is formed inside the diverging nozzle and Mach exit is

subsonic. This explains why at PR = 4.97 the noise level drops. Then, increasing PR further, the noise increases again but with a higher power law then the other valves.

Comparing with the semi-empirical model (solid lines), in the middle PR range the agreement is very good, apart from valve 1, but at the highest PRs, for the biggest valves (5 and 6) the model generally underpredicts the noise, while for the smallest valve (2) it overpredicts the level. The difference is most significant for the smallest valves, being about 4 dB, while is only 2 dB for the biggest valves.

The major discrepancy between the semi-empirical model and the experimental data is at the lowest PRs when the valve is not choked and only the turbulent mixing noise (Eq. 2) is included in the model. The slope of the experimental data follows more the intermediate regime and this is consistent for all valve sizes, suggesting that at lower PRs when $M_{jet} < 1$ but approaching 1, the turbulent mixing noise model is not suitable to account for the actual total noise mechanism especially for bigger valves.

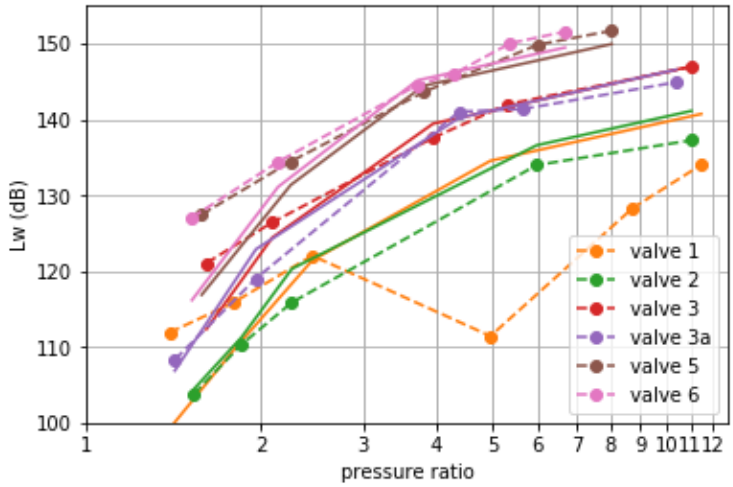

Figure 3: Experimental overall levels per valve (dashed lines) compared with the valve model (solid lines) plotted versus PR.

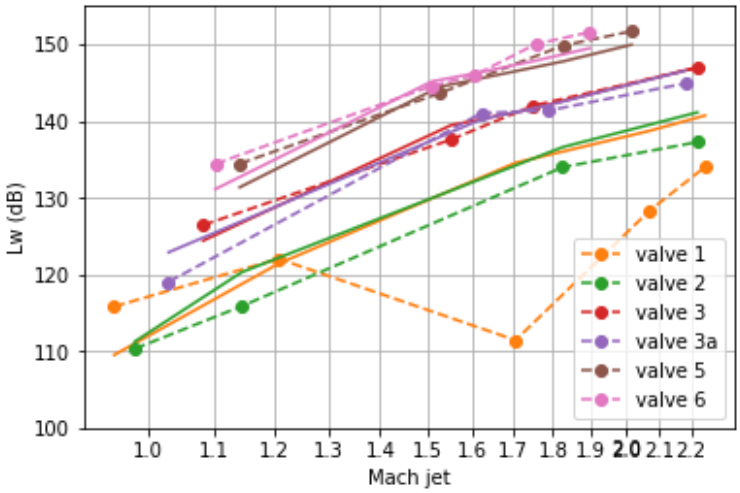

Figure 4: Experimental overall levels per valve (dashed lines) compared with the valve model (solid lines) plotted versus M_{jet}.

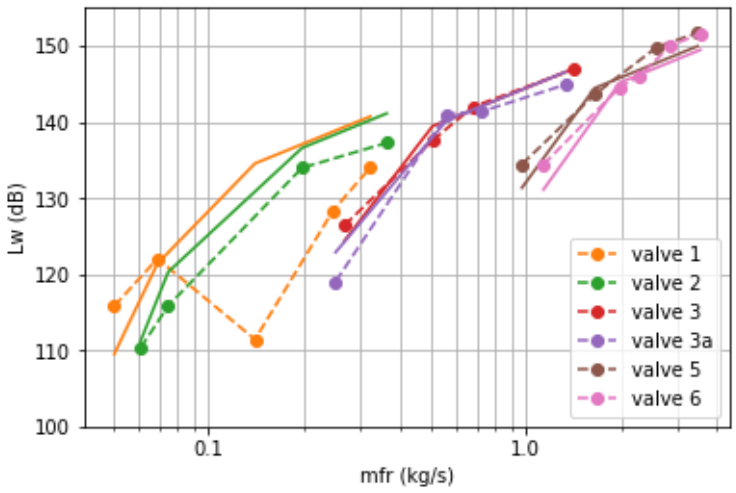

Figure 5: Experimental overall levels per valve (dashed lines) compared with the valve model (solid lines) plotted versus $\dot{m}_{exit}$.

5. IMPLICATIONS FOR EXTRAPOLATION

The classical 8th power scaling law based on M_{jet} defined for jet noise can be applied to the overall levels plotted in Figure 4. Because M_{jet} does not account for valve size, three different trendlines have been fitted to the data corresponding to the three main sizes, as shown in Figure 6.

However, because $\dot{m}_{exit}$ depends on the valve size, it is possible to fit a single trendline to interpolate over all the valves for the highest values, as shown in Figure 7. In this case the best fit slope for the trendline follows the power law of 1.5, so that the line plotted in Figure 7 is:

$$L_w = 145 + 1.5 * 10\ \log(\dot{m}_{exit}) \qquad (12)$$

This 1.5 power law is a small adjustment to the power law of 1.7 that can be derived from the shock noise model at the highest M_{jet} as described in [1].

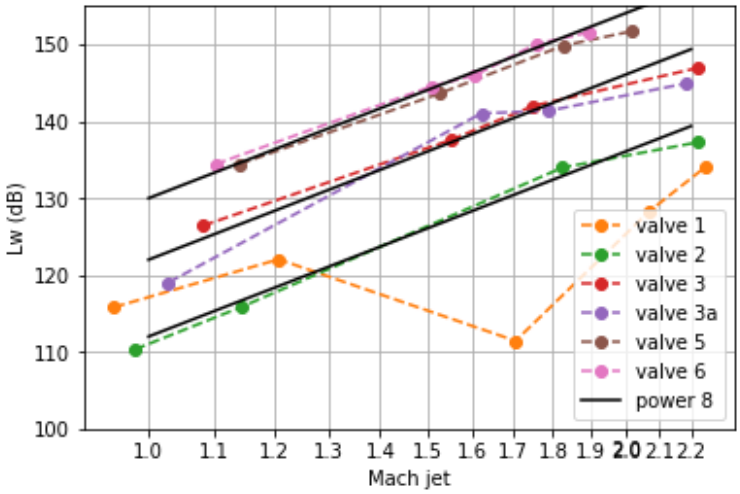

Figure 6: Fitting a trendline per valve size type using a power law of 8.

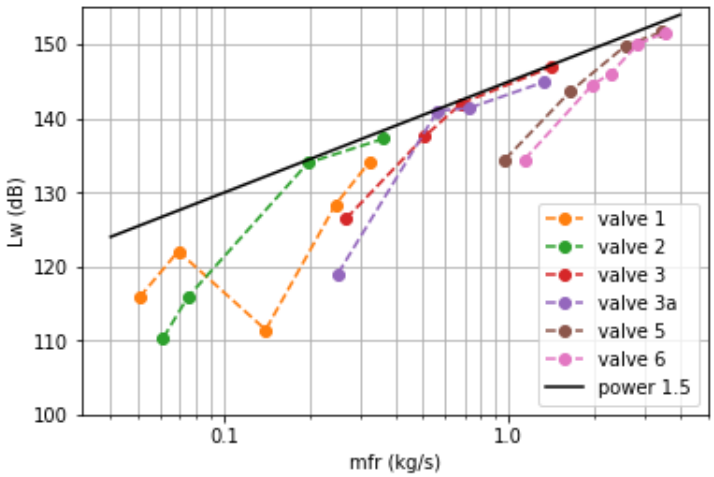

Figure 7: Fitting a trendline using a power law of 1.5 to extrapolate at the higher $\dot{m}_{exit}$ over all the valves.

6. CONCLUSIONS

Tests of six valves were carried out over a range of flow conditions shown in Table 1. These data may be interpolated to give noise levels for specific flow conditions. The main question addressed by the paper is how these data compare with the semi-empirical model available in the literature and if the model can be extended to extrapolate the noise level to higher PR and mass flow.

Analysis of the noise spectra showed that in choked conditions the peak frequency broadly decreases with PR, as predicted by the model. Noise levels vary with the classical law of the 8th power of jet Mach number for valves 2-6. However, valve 1 behaved differently because the nozzle is converging–diverging, so that choking occurs inside the valve rather than at the exit. For the other valves the detailed shape does not affect the overall noise level, which only depends on the main nozzle diameter.

Considering data for all the valves, at the lowest mass flow rate, when approaching the choking condition, the turbulent mixing mechanism does not seem to be sufficient to give the correct scaling law. In the higher range a scaling law of sound power increasing as mass flow rate to the power 1.5 has been derived. This is a small adjustment to the valve model described in the literature, but seems to be more appropriate to extrapolate to higher PR for all valve types.

7. REFERENCES

1 Beranek, L. *Noise and vibration control*, Institute of Noise and Control Engineering, Washington DC, USA, 1988

2 Cantwell, B.J. *Fundamentals of Compressible Flow*, Stanford University CA, USA, 3 October 2018.